NATIONAL ADVISORY COMMITTEE FOR AERONAUTICS

TECHNICAL NOTE 2470

EFFECT OF AN AUTOPILOT SENSITIVE TO YAWING VELOCITY

ON THE LATERAL STABILITY OF A TYPICAL

HIGH-SPEED AIRPLANE

By Ordway B. Gates, Jr., and Leonard Sternfield

Langley Aeronautical Laboratory
Langley Field, Va.

NACA

Washington
September 1951

NATIONAL ADVISORY COMMITTEE FOR AERONAUTICS

TECHNICAL NOTE 2470

EFFECT OF AN AUTOPILOT SENSITIVE TO YAWING VELOCITY

ON THE LATERAL STABILITY OF A TYPICAL

HIGH-SPEED AIRPLANE

By Ordway B. Gates, Jr., and Leonard Sternfield

SUMMARY

A theoretical investigation has been made to determine the effect
on the lateral stability of a typical high-speed fighter airplane of an
autopilot sensitive to yawing velocity. The effects of inclination of
the gyro spin axis to the flight path and of time lag in the autopilot
were also determined. The flight conditions investigated included
landing at sea level, approach condition at 12,000 feet, and cruising at
50,000 feet at Mach numbers of 0.80 and 1.2. The results of the inves-
tigation indicated that the lateral stability characteristics of the
airplane equipped with this autopilot should satisfy the period-damping
criterion. Airplane motions subsequent to a disturbance in sideslip
are presented for several representative flight conditions in which a
time lag in the autopilot of 0.10 second was assumed.

INTRODUCTION

Recent flight tests of aircraft designed for transonic and super-
sonic speeds have indicated that poorly damped lateral oscillations are
encountered. A means for providing adequate damping of such oscillations
is therefore desirable. The results presented in reference 1 show that
the damping of the lateral oscillation of an airplane can be improved by
use of automatic stabilization, and the type of autopilot which resulted
in the greatest improvement in damping was found to be one which applies
rudder control proportional to the yawing angular velocity. Such an
autopilot was installed in the Boeing XB-47 and, according to reference 2,
the flight tests of this airplane with the autopilot installed indicated
an increase in the damping of the lateral oscillation. The purpose of
the present investigation is to determine the effect of this type of
autopilot on the lateral stability of a typical fighter airplane designed
for transonic and supersonic speeds.

The effects on the lateral stability characteristics of inclination of the gyro spin axis to the flight path and of time lag in the autopilot system are also discussed. The results of the investigation are presented in the form of motions subsequent to an initial disturbance in sideslip and plots of the time to damp to half-amplitude and the period of the oscillation for different flight conditions.

SYMBOLS AND COEFFICIENTS

ϕ angle of roll, radians

ψ angle of yaw, radians

β angle of sideslip, radians (v/V)

$r,\dot{\psi}$ yawing angular velocity, radians per second $(d\psi/dt)$

$p,\dot{\phi}$ rolling angular velocity, radians per second $(d\phi/dt)$

v sideslip velocity along lateral axis, feet per second

V airspeed, feet per second

ρ mass density of air, slugs per cubic foot

q dynamic pressure, pounds per square foot $\left(\frac{1}{2}\rho V^2\right)$

b wing span, feet

S_W wing area, square feet

S_A auxiliary-control-surface area

S_R rudder area

W weight of airplane, pounds

m mass of airplane, slugs (W/g)

g acceleration due to gravity, feet per second per second

μ_b relative-density factor $(m/\rho S_W b)$

ϵ angle between longitudinal body axis and principal axis, positive when body axis is above principal axis at nose, degrees

η inclination of principal longitudinal axis of airplane with respect to flight path, positive when principal axis is above flight path at nose, degrees $(\alpha - \epsilon)$

γ angle of flight path to horizontal axis, positive in climb, degrees

k_{X_O} radius of gyration in roll about principal longitudinal axis, feet

k_{Z_O} radius of gyration in yaw about principal vertical axis, feet

K_{X_O} nondimensional radius of gyration in roll about principal longitudinal axis $\left(k_{X_O}/b\right)$

K_{Z_O} nondimensional radius of gyration in yaw about principal vertical axis $\left(k_{Z_O}/b\right)$

K_X nondimensional radius of gyration in roll about longitudinal stability axis $\left(\sqrt{K_{X_O}^2\cos^2\eta + K_{Z_O}^2\sin^2\eta}\right)$

K_Z nondimensional radius of gyration in yaw about vertical stability axis $\left(\sqrt{K_{Z_O}^2\cos^2\eta + K_{X_O}^2\sin^2\eta}\right)$

K_{XZ} nondimensional product-of-inertia parameter $\left(\left(K_{Z_O}^2 - K_{X_O}^2\right)\sin\eta\,\cos\eta\right)$

C_L trim lift coefficient $\left(\dfrac{W\cos\gamma}{qS}\right)$

C_l rolling-moment coefficient $\left(\dfrac{\text{Rolling moment}}{qSb}\right)$

C_n yawing-moment coefficient $\left(\dfrac{\text{Yawing moment}}{qSb}\right)$

C_Y lateral-force coefficient $\left(\dfrac{\text{Lateral force}}{qS}\right)$

$$C_{l_\beta} = \frac{\partial C_l}{\partial \beta} \qquad\qquad C_{l_p} = \frac{\partial C_l}{\partial \frac{pb}{2V}} \qquad\qquad C_{l_r} = \frac{\partial C_l}{\partial \frac{rb}{2V}}$$

$$C_{n_\beta} = \frac{\partial C_n}{\partial \beta} \qquad\qquad C_{n_p} = \frac{\partial C_n}{\partial \frac{pb}{2V}} \qquad\qquad C_{n_r} = \frac{\partial C_n}{\partial \frac{rb}{2V}}$$

$$C_{Y_\beta} = \frac{\partial C_Y}{\partial \beta} \qquad\qquad C_{Y_p} = \frac{\partial C_Y}{\partial \frac{pb}{2V}} \qquad\qquad C_{Y_r} = \frac{\partial C_Y}{\partial \frac{rb}{2V}}$$

t time, seconds

s_b nondimensional time parameter based on span (Vt/b)

D_b differential operator $\left(\frac{d}{ds_b}\right)$

P period of oscillation, seconds

$T_{1/2}$ time for amplitude of oscillation to damp to one-half its original value

T_2 time for amplitude of oscillation to double its original value

a real part of complex root of characteristic stability equation

ω angular frequency, radians per second

$\omega_s = \frac{b}{V} \omega$

$\lambda = a \pm i\omega_s$

τ time lag between signal for control and its actual motion, seconds

δ_A deflection of the auxiliary control surface, radians

$$\left. \begin{array}{l} C_{n_{\delta_A}} = \dfrac{\partial C_n}{\partial \delta_A} \\[3em] C_{l_{\delta_A}} = \dfrac{\partial C_l}{\partial \delta_A} \end{array} \right\} \quad \text{control-effectiveness parameters}$$

α angle of attack with respect to longitudinal body axis, degrees (See fig. 1.)

Φ inclination of gyro reference axis to longitudinal body axis, degrees (See fig. 1.)

ξ inclination of gyro reference axis to longitudinal stability or flight-path axis, degrees (See fig. 1.)

ΔC_{n_r} increment of C_{n_r} due to the autopilot

ΔC_{n_p} increment of C_{n_p} due to the autopilot

ΔC_{l_r} increment of C_{l_r} due to the autopilot

ΔC_{l_p} increment of C_{l_p} due to the autopilot

$\dot{\psi}_{GA}$ yawing velocity about an axis perpendicular to gyro reference axis, radians per second $\left(\dot{\psi}_{GA} = \dot{\psi}_{SA} \cos \xi + \dot{\phi}_{SA} \sin \xi \right)$

$$\left(D_b \psi \right)_{GA} = \frac{b}{V} \dot{\psi}_{GA} = D_b \psi_{SA} \cos \xi + D_b \phi_{SA} \sin \xi$$

K control gearing ratio $\left(\dfrac{\partial \delta_A}{\partial \dot{\psi}} \right)_{GA}$

$C_{L_{\delta_A}}$ lift per unit deflection of auxiliary control surface

l distance from center of gravity of airplane to center of
pressure of auxiliary control surface, feet

h distance from airplane longitudinal body axis to center of
pressure of auxiliary control surface, feet

Subscripts:

GA autopilot, gyro axis

SA stability axis

BA airplane body axis

A auxiliary control surface

R rudder

ANALYSIS

Equations of motion.- The linearized equations of motion, referred
to stability axes, for the condition of controls fixed are:

Rolling

$$2\mu_b\left(K_X{}^2 D_b{}^2\phi + K_{XZ}D_b{}^2\psi\right) = C_{l_\beta}\beta + \frac{1}{2}C_{l_p}D_b\phi + \frac{1}{2}C_{l_r}D_b\psi$$

Yawing

$$2\mu_b\left(K_Z{}^2 D_b{}^2\psi + K_{XZ}D_b{}^2\phi\right) = C_{n_\beta}\beta + \frac{1}{2}C_{n_p}D_b\phi + \frac{1}{2}C_{n_r}D_b\psi$$

Sideslipping

$$2\mu_b\left(D_b\beta + D_b\psi\right) = C_{Y_\beta}\beta + \frac{1}{2}C_{Y_p}D_b\phi + C_L\phi + \frac{1}{2}C_{Y_r}D_b\psi + \left(C_L \tan \gamma\right)\psi$$

When $\phi_0 e^{\lambda s_b}$ is substituted for ϕ, $\psi_0 e^{\lambda s_b}$ for ψ, and $\beta_0 e^{\lambda s_b}$ for β in the equations written in determinant form (where ϕ_0, ψ_0, and β_0 refer to the constant coefficients in the solution for ϕ, ψ, and β, respectively), λ must be a root of the stability equation

$$A\lambda^4 + B\lambda^3 + C\lambda^2 + D\lambda + E = 0 \tag{1}$$

where

$$A = 8\mu_b^3\left(K_X^2 K_Z^2 - K_{XZ}^2\right)$$

$$B = -2\mu_b^2\left(2K_X^2 K_Z^2 C_{Y_\beta} + K_X^2 C_{n_r} + K_Z^2 C_{l_p} - 2K_{XZ}^2 C_{Y_\beta} - K_{XZ}C_{l_r} - K_{XZ}C_{n_p}\right)$$

$$C = \mu_b\left(K_X^2 C_{n_r}C_{Y_\beta} + 4\mu_b K_X^2 C_{n_\beta} + K_Z^2 C_{l_p}C_{Y_\beta} + \tfrac{1}{2}C_{n_r}C_{l_p} - K_{XZ}C_{l_r}C_{Y_\beta} - \right.$$

$$4\mu_b K_{XZ}C_{l_\beta} - \tfrac{1}{2}C_{n_p}C_{l_r} - C_{n_p}K_{XZ}C_{Y_\beta} + K_{XZ}C_{n_\beta}C_{Y_p} - K_Z^2 C_{Y_p}C_{l_\beta} -$$

$$\left. K_X^2 C_{Y_r}C_{n_\beta} + K_{XZ}C_{Y_r}C_{l_\beta}\right)$$

$$D = -\tfrac{1}{4}C_{n_r}C_{l_p}C_{Y_\beta} - \mu_b C_{l_p}C_{n_\beta} + \tfrac{1}{4}C_{n_p}C_{l_r}C_{Y_\beta} + \mu_b C_{n_p}C_{l_\beta} + 2\mu_b C_L K_{XZ}C_{n_\beta} -$$

$$2\mu_b C_L K_Z^2 C_{l_\beta} - 2\mu_b K_X^2 C_{n_\beta}C_L \tan\gamma + 2\mu_b K_{XZ}C_{l_\beta}C_L \tan\gamma + \tfrac{1}{4}C_{l_p}C_{n_\beta}C_{Y_r} -$$

$$\tfrac{1}{4}C_{n_p}C_{l_\beta}C_{Y_r} - \tfrac{1}{4}C_{l_r}C_{n_\beta}C_{Y_p} + \tfrac{1}{4}C_{n_r}C_{l_\beta}C_{Y_p}$$

$$E = \tfrac{1}{2}C_L\left(C_{n_r}C_{l_\beta} - C_{l_r}C_{n_\beta}\right) + \tfrac{1}{2}C_L \tan\gamma\left(C_{l_p}C_{n_\beta} - C_{n_p}C_{l_\beta}\right)$$

The damping and period of the lateral oscillation in seconds are given by the equations

$$T_{1/2} = -\frac{0.693}{a}\frac{b}{V} \qquad a < 0$$

$$T_2 = \frac{0.693}{a}\frac{b}{V} \qquad a > 0$$

$$P = \frac{6.28}{\omega_s}\frac{b}{V}$$

where a and ω_s are the real and imaginary parts of a complex root of stability equation (1).

Stability derivatives contributed by autopilot.- In order to analyze the effect on the lateral stability of an airplane of installing an auto-pilot sensitive to rate of yaw, the derivation of equations describing the increments to the stability derivatives which must be included in the equations of motion is necessary. The system of axes employed in the derivations is shown in figure 1. Since the equations of motion are derived with respect to the stability axes, the autopilot derivatives must also be related to the stability axes. The autopilot, through use of an auxiliary rudder surface, introduces a yawing moment about the vertical body axis and a rolling moment about the longitudinal body axis, both of which are proportional to the rate of yaw with respect to an axis perpendicular to the gyro reference axis; that is,

$$\left(C_n\right)_{BA} = C_{n_{\delta_A}}\delta_A = C_{n_{\delta_A}}\frac{\partial \delta_A}{\partial\left(D_b\psi\right)_{GA}}\left(D_b\psi\right)_{GA}$$

$$\left(C_l\right)_{BA} = C_{l_{\delta_A}}\delta_A = C_{l_{\delta_A}}\frac{\partial \delta_A}{\partial\left(D_b\psi\right)_{GA}}\left(D_b\psi\right)_{GA}$$

Now,

$$\left(D_b\psi\right)_{GA} = \left(D_b\psi\right)_{SA}\cos\xi + \left(D_b\phi\right)_{SA}\sin\xi$$

$$\left(C_n\right)_{SA} = \left(C_n\right)_{BA} \cos\alpha - \left(C_l\right)_{BA} \sin\alpha$$

$$\left(C_l\right)_{SA} = \left(C_l\right)_{BA} \cos\alpha + \left(C_n\right)_{BA} \sin\alpha$$

Therefore, by substitution

$$\left(C_n\right)_{SA} = \left(C_{n_{\delta_A}} \cos\alpha - C_{l_{\delta_A}} \sin\alpha\right) K \frac{V}{b}\left[\left(D_b\psi\right)_{SA} \cos\xi + \left(D_b\phi\right)_{SA} \sin\xi\right]$$

$$\left(C_l\right)_{SA} = \left(C_{l_{\delta_A}} \cos\alpha + C_{n_{\delta_A}} \sin\alpha\right) K \frac{V}{b}\left[\left(D_b\psi\right)_{SA} \cos\xi + \left(D_b\phi\right)_{SA} \sin\xi\right]$$

where $K = \dfrac{\partial\delta_A}{\partial(\dot\psi)_{GA}}$. The angles ξ and α are assumed to be small. Thus, the usual simplification is made that the sine of a small angle is equal to the angle in radians and the cosine is equal to unity. The preceding equations therefore become

$$\left.\begin{aligned}
\left(C_n\right)_{SA} &= \left(C_{n_{\delta_A}} - \alpha C_{l_{\delta_A}}\right) K \frac{V}{b}\left[\left(D_b\psi\right)_{SA} + \xi\left(D_b\phi\right)_{SA}\right] \\[2ex]
\left(C_l\right)_{SA} &= \left(C_{l_{\delta_A}} + \alpha C_{n_{\delta_A}}\right) K \frac{V}{b}\left[\left(D_b\psi\right)_{SA} + \xi\left(D_b\phi\right)_{SA}\right]
\end{aligned}\right\} \qquad (2)$$

Equations (2) may be written in the form

$$\left(C_n\right)_{SA} = \frac{\partial C_n}{\partial\left(D_b\psi\right)_{SA}}\left(D_b\psi\right)_{SA} + \frac{\partial C_n}{\partial\left(D_b\phi\right)_{SA}}\left(D_b\phi\right)_{SA}$$

$$\left(C_l\right)_{SA} = \frac{\partial C_l}{\partial\left(D_b\psi\right)_{SA}}\left(D_b\psi\right)_{SA} + \frac{\partial C_l}{\partial\left(D_b\phi\right)_{SA}}\left(D_b\phi\right)_{SA}$$

where

$$\frac{\partial C_n}{\partial(D_b\psi)_{SA}} = K\,\frac{V}{b}\left(C_{n\delta_A} - \alpha C_{l\delta_A}\right) = \frac{1}{2}\,\Delta C_{n_r}$$

$$\frac{\partial C_n}{\partial(D_b\phi)_{SA}} = K\,\frac{V}{b}\left(C_{n\delta_A} - \alpha C_{l\delta_A}\right)\xi = \frac{1}{2}\,\Delta C_{n_p}$$

$$\frac{\partial C_l}{\partial(D_b\psi)_{SA}} = K\,\frac{V}{b}\left(C_{l\delta_A} + \alpha C_{n\delta_A}\right) = \frac{1}{2}\,\Delta C_{l_r}$$

$$\frac{\partial C_l}{\partial(D_b\phi)_{SA}} = K\,\frac{V}{b}\left(C_{l\delta_A} + \alpha C_{n\delta_A}\right)\xi = \frac{1}{2}\,\Delta C_{l_p}$$

Thus

$$\left.\begin{aligned}
\Delta C_{n_r} &= 2K\,\frac{V}{b}\left(C_{n\delta_A} - \alpha C_{l\delta_A}\right)\\[2ex]
\Delta C_{n_p} &= 2K\,\frac{V}{b}\left(C_{n\delta_A} - \alpha C_{l\delta_A}\right)\xi = \Delta C_{n_r}\xi\\[2ex]
\Delta C_{l_r} &= 2K\,\frac{V}{b}\left(C_{l\delta_A} + \alpha C_{n\delta_A}\right)\\[2ex]
\Delta C_{l_p} &= 2K\,\frac{V}{b}\left(C_{l\delta_A} + \alpha C_{n\delta_A}\right)\xi = \Delta C_{l_r}\xi
\end{aligned}\right\} \qquad (3)$$

The control effectiveness parameters $C_{n_{\delta_A}}$ and $C_{l_{\delta_A}}$ of the auxiliary rudder surface are given by the expressions

$$
\left.
\begin{aligned}
C_{n_{\delta_A}} &= -C_{L_{\delta_A}} \frac{S_A}{S_W} \frac{l}{b} \\[2ex]
C_{l_{\delta_A}} &= C_{L_{\delta A}} \frac{S_A}{S_W} \frac{h}{b} = -\frac{h}{l} C_{n_{\delta_A}}
\end{aligned}
\right\} \tag{4}
$$

Values for the derivative $C_{L_{\delta_A}}$ were estimated from unpublished theoretical results based on the Weissinger lifting-surface theory. When these expressions for $C_{n_{\delta_A}}$ and $C_{l_{\delta_A}}$ are substituted in equations (3) the following equations result:

$$
\left.
\begin{aligned}
\Delta C_{n_r} &= -2K \frac{V}{b} C_{L_{\delta_A}} \frac{S_A}{S_W} \frac{l}{b}\left(1 + \frac{h\alpha}{l}\right) \\[2ex]
\Delta C_{n_p} &= -2K \frac{V}{b} C_{L_{\delta_A}} \frac{S_A}{S_W} \frac{l}{b} \xi\left(1 + \frac{h\alpha}{l}\right) = \xi\,\Delta C_{n_r} \\[2ex]
\Delta C_{l_r} &= -2K \frac{V}{b} C_{L_{\delta_A}} \frac{S_A}{S_W} \frac{l}{b}\left(\alpha - \frac{h}{l}\right) \\[2ex]
\Delta C_{l_p} &= -2K \frac{V}{b} C_{L_{\delta_A}} \frac{S_A}{S_W} \frac{l}{b} \xi\left(\alpha - \frac{h}{l}\right) = \xi\,\Delta C_{l_r}
\end{aligned}
\right\} \tag{5}
$$

The values of the derivatives C_{n_r}, C_{n_p}, C_{l_r}, and C_{l_p} which appear in the stability equations must be modified therefore to include the increments ΔC_{n_r}, ΔC_{n_p}, ΔC_{l_r}, and ΔC_{l_p}.

For this investigation a further assumption has been made that the center of pressure of the auxiliary surface is located a negligible distance from the fuselage center line; that is, h is approximately

equal to zero. Also, the product $\xi\alpha$ is considered to be of second order and terms involving this product have been neglected.

Equations (5) become therefore:

$$\Delta C_{n_r} = -2K \frac{V}{b} C_{L_{\delta_A}} \frac{S_A}{S_W} \frac{l}{b}$$

$$\Delta C_{n_p} = -2K \frac{V}{b} C_{L_{\delta_A}} \frac{S_A}{S_W} \frac{l}{b} \xi = \xi \Delta C_{n_r}$$

$$\Delta C_{l_r} = -2K \frac{V}{b} C_{L_{\delta_A}} \frac{S_A}{S_W} \frac{l}{b} \alpha = \alpha \Delta C_{n_r}$$

$$\Delta C_{l_p} = 0$$

$$(6)$$

The derivative $C_{L_{\delta_A}}$ is algebraically positive; therefore, when ξ is a negative angle (that is, for the gyro reference axis below the flight path), ΔC_{n_p} is positive. Similarly, when α is negative, ΔC_{l_r} is positive. It will be shown in a subsequent section entitled "Results and Discussion" that the term ΔC_{l_r} has only a negligible effect on the damping of the lateral oscillation of the airplane and was therefore omitted in the analysis.

If the location of the auxiliary surface is such as to make the assumption $h = 0$ invalid, the increments to the stability derivatives should be calculated from equations (5).

RESULTS AND DISCUSSION

The present investigation was undertaken to determine whether an autopilot sensitive to rate of yaw would satisfactorily improve the inherently poor lateral stability characteristics of a typical high-speed fighter airplane. The motion in sideslip of such an airplane subsequent to a rudder deflection of 10° in flight for a simulated landing condition at 12,000 feet is shown in figure 2. The landing gear

and flaps were extended. The mass and aerodynamic characteristics for this flight condition and other conditions considered to be representative of this type of aircraft are presented in table I. The motion of figure 2 is approximately undamped $(T_{1/2} = 100 \text{ sec})$ and has a period of 2.5 seconds.

If the assumption is made that the autopilot gyro axis is alined with the longitudinal stability axis, the autopilot effectively only introduces the derivative ΔC_{n_r}. As indicated in a previous section entitled "Stability derivatives contributed by autopilot," the expression for ΔC_{n_r} is a function of two parameters, $\dfrac{S_A}{S_W}$ and the control gearing ratio K, which may be arbitrarily selected by the designer. It was therefore necessary first to determine the value of ΔC_{n_r} which would give satisfactory lateral stability and then to determine the combinations of $\dfrac{S_A}{S_W}$ and K which would result in that prescribed value of ΔC_{n_r}.

The criterion for satisfactory lateral stability as specified in reference 3 is shown in figure 3. The time required for the amplitude of the oscillation to be reduced to one-half its original value $T_{1/2}$ is plotted against the period P. For the flight condition described previously, the value of $C_{n_r} = -1.0$. The period-damping relationship of the airplane for this value of C_{n_r} is located on the unsatisfactory side of the boundary. The period for the basic flight condition, as pointed out before, is 2.5 seconds and $T_{1/2}$ is about 100 seconds. When C_{n_r} was increased to -2.0, that is, $\Delta C_{n_r} = -1.0$, the period-damping relationship almost exactly satisfied the criterion. For $\Delta C_{n_r} = -2.0$, the relationship is such as to fall well into the acceptable range. Thus, for $\Delta C_{n_r} = -1.0$ or -2.0, the period-damping relationship of this airplane would be satisfactory.

A theoretical analysis was made therefore to determine the amount of auxiliary area necessary to give these increments of C_{n_r} for different gearing ratios of the autopilot. The results of this analysis are presented in figure 4. The ratio $\dfrac{S_A}{S_R}$ has been used as an ordinate instead of $\dfrac{S_A}{S_W}$, since a part of the rudder surface is assumed to be used as the auxiliary control surface.

The combinations of gearing ratio and auxiliary area which would result in a $\Delta C_{n_r} = -2.0$ for the previously described flight condition (condition I, table I) are given by the curve $\Delta C_{n_r} = -2.0$. For the gearing ratio of 2 to 1 which was selected for the subsequent analysis, the required area is approximately 20 percent of the rudder area. This gearing ratio of 2 to 1 means that the auxiliary surface will be deflected 2° for a rate of yaw of 1° per second. For the rates of yaw encountered on this airplane, this value for the gearing ratio is reasonable. The value of ΔC_{n_r} obtained by use of a specific auxiliary surface will be different for other flight conditions since its magnitude varies directly with airspeed. (See equation (6).)

Effect of inclination of the gyro axis.- The assumption was made in the preceding analysis that the autopilot gyro axis was alined with the flight path or longitudinal stability axis. Since the equations of motion are derived with respect to the stability axes, the autopilot was in effect increasing only the stability derivative C_{n_r}. For this type of autopilot the angularity between the longitudinal body-axis and the gyro spin axis, once fixed, is preserved for all flight conditions and therefore the gyro axis is alined with the flight path for only one angle of attack.

For any flight condition where the gyro axis is not alined with the flight path, that is, $\xi \neq 0$, the autopilot is sensitive to both yawing and rolling velocities about the stability axes. Hence, an increment to the yawing moment proportional to rolling velocity about the stability axes must also be introduced into the equations of motion. This additional yawing moment due to rolling velocity is in effect an increment in the stability derivative C_{n_p}.

This derivative C_{n_p} has been shown to have an important effect on the damping of the lateral oscillation (references 4 and 5). If ΔC_{n_p} is algebraically positive it will have a stabilizing effect provided it is not allowed to become excessively large. If ΔC_{n_p} becomes too large a positive quantity, another oscillation which becomes less stable with further increases in ΔC_{n_p} will be introduced.

Calculations taking into account the derivative C_{n_p} were made for the four flight conditions described in table I in order to determine a value for the angle Φ (see fig. 1) which would be satisfactory throughout the range of likely flight conditions. Numerous values of the angle Φ were investigated and the results are presented in figure 5. The period of the oscillatory mode P and the time to damp to half-amplitude $T_{1/2}$

in seconds are plotted against the angle ϕ in degrees. For the flight condition at 12,000 feet (fig. 5(a)) the damping of the original oscillatory mode, denoted by $(T_{1/2})_1$, continues to improve as ϕ is increased in the positive direction. The period of this mode increases slightly as ϕ is increased to 2^9, but beyond this value it becomes somewhat less. For a value of ϕ approximately equal to 2° a second oscillatory mode is introduced into the system. The damping and period of this mode are shown as $(T_{1/2})_2$ and P_2, respectively. For $\phi > 2^o$ this second oscillation becomes rapidly less stable and for $\phi > 8^o$ this mode is unstable. The period of this second oscillation at first decreases, but for $\phi > 3^o$ the trend is reversed and the period becomes longer for further increases in ϕ. The formation of this second oscillation and its subsequent decrease in stability with increases in ϕ is due to the large positive values of the derivative ΔC_{n_p}. The period of this second oscillation is, in general, much longer than that of the original oscillation.

For the landing condition at sea level (fig. 5(b)), the damping of the lateral oscillation continues to improve with increases in ϕ, while the period increases only very slightly. For the range of ϕ investigated a second oscillation was not introduced. The results for the subsonic condition at 50,000 feet are shown in figure 5(c). As ϕ is increased, the damping of the original oscillation improves considerably; while the period of this oscillation is relatively unchanged. For $\phi > 5^o$ a second oscillation is introduced which becomes rapidly less stable for further increases in ϕ. The period of this mode continues to decrease for the range of ϕ investigated. For the supersonic condition at 50,000 feet (fig. 5(d)), the same trends are noted for the oscillation which is present for $\phi = 0^o$ as were noted for the same oscillation in the subsonic condition; that is, the damping becomes greater as ϕ is increased and the period is relatively unchanged. For $\phi > 5^o$, a second oscillatory mode again is introduced which becomes less stable for larger values of ϕ. The results shown in these figures indicate that the damping of the lateral oscillation will be satisfactory for all the conditions discussed if ϕ is between 0° and 5.2^o.

Effect of time lag in the autopilot on the airplane motions.- An experimental frequency-response investigation of an autopilot similar to the one discussed in this paper indicated that the assumption of a constant time lag may be justified. The time lag for the experimentally investigated autopilot was found to be less than 0.10 second. The effect of a time lag in the autopilot of 0.10 second on the lateral stability of the airplane was determined by the methods of reference 6 and was found to be negligible. In order to verify this result, the airplane motion in sideslip subsequent to a disturbance in sideslip of 5° was calculated for each of the flight conditions discussed previously and a time lag of 0.10 second was taken into account. The motions, which

were calculated by using a step-by-step procedure, were obtained for
two values of the angle ϕ, -2° and 5°, and the results are presented
in figure 6. The values of $T_{1/2}$ and P as determined from these
curves are almost identical with the value for the corresponding flight
conditions as shown in figure 5 for which zero time lag was assumed.
For $\phi = 5.2^\circ$, the presence of a secondary oscillatory mode can be
detected in the flight condition at 12,000 feet and in the high-speed
condition at 50,000 feet. Also, for $\phi = -2^\circ$, the damping of the oscill-
ation for the landing condition at sea level and the subsonic case at
50,000 feet barely satisfies the damping criterion of reference 3.

Effect of ΔC_{l_r}.- The autopilot derivative ΔC_{l_r} was discussed in
a previous section and was assumed to be negligible in the present
analysis. In order to justify this assumption, the motion for $\phi = 5.2^\circ$
for the subsonic case at 50,000 feet was calculated by taking into
account the derivative ΔC_{l_r} as defined in equations (6). Points on
the resulting curve are shown in figure 6 for condition III. It is readily
seen that the derivative ΔC_{l_r} has no effect on the motion for this
case.

Additional calculations.- The assumption was made in the previous
analysis that the center of pressure of the auxiliary surface was located
on the fuselage center line, that is, $\frac{h}{b} = 0$. In order to determine the
effect of locating the surface at a position above the fuselage center
line, some additional calculations were made for the center of pressure
of the surface 6 feet above the fuselage center line $\left(\frac{h}{b} = 0.24\right)$. Several
inclinations of the gyro spin axis were investigated for each of the
flight conditions discussed previously and the increments to the stability
derivatives C_{n_r}, C_{n_p}, C_{l_r}, and C_{l_p} were calculated from equa-
tions (5). A comparison of the values of $T_{1/2}$ and P obtained for
these two center-of-pressure locations is presented in table II. The
values of ΔC_{n_r} and ΔC_{n_p} were assumed to be the same for both center-
of-pressure locations for each gyro-axis inclination since the term $\frac{h\alpha}{l}$
in equations (5) is negligible when it is compared with unity. In
general, the results for both center-of-pressure locations show the same
trends. For $\frac{h}{b} = 0.24$ the spiral mode $\left(T_{1/2}\right)_1$ is less stable than
was indicated by the results for $\frac{h}{b} = 0$. The formation of the second
oscillatory mode for each condition investigated occurs at higher values
of ϕ for the high center-of-pressure location than for the cases where
$\frac{h}{b} = 0$. The decrease in spiral stability is due primarily to the large

positive values of ΔC_{l_r}; whereas the delay in the formation of the additional oscillatory mode is due to both the large positive value of ΔC_{l_r} and the negative values of ΔC_{l_p}. For the values of ϕ which resulted in small values of ΔC_{l_p}, the period and damping of the oscilatory mode were only slightly affected even though ΔC_{l_r} was large. For example, the value of ΔC_{l_r} for condition IV is approximately ten times as large as the C_{l_r} of the airplane, but for $\phi = 2^o$, where $\Delta C_{l_p} = -0.03$, the only significant effect is on the spiral stability.

The general effect of locating the surface above the fuselage center line is to shift the curves of figure 5 along the ϕ axis in the positive direction. As a result, the range of ϕ for which the stability of the lateral oscillation will be satisfactory is extended to include higher values of ϕ than for the case of $\frac{h}{b} = 0$. For this particular center-of-pressure location, an inclination of the gyro axis of as much as 10° will result in satisfactory stability.

<div align="center">CONCLUSIONS</div>

The following conclusions were reached from a theoretical analysis of the effect on the lateral stability of a typical high-speed airplane of an autopilot sensitive to rate of yaw:

1. The damping of the lateral oscillation of the airplane studied for all the flight conditions discussed should satisfy the Air Force - Navy criterion when the proposed autopilot is installed.

2. When the effect of a rate gyro on the lateral stability of a particular airplane is analyzed it is important to take into account the inclination of the gyro spin axis to the flight path. For the case of $\frac{h}{b} = 0$, values of ϕ between 0° and 5° were satisfactory for the configurations considered; whereas, for $\frac{h}{b} = 0.24$, values up to 10° resulted in satisfactory stability.

3. A time lag in the autopilot of 0.10 second had a negligible effect on the calculated lateral stability of the airplane analyzed.

Langley Aeronautical Laboratory
    National Advisory Committee for Aeronautics
        Langley Field, Va., June 27, 1950

REFERENCES

1. Sternfield, Leonard: Effect of Automatic Stabilization on the Lateral
   Oscillatory Stability of a Hypothetical Airplane at Supersonic
   Speeds. NACA TN 1818, 1949.

2. White, Roland J.:   Investigation of Lateral Dynamic Stability in the
   XB-47 Airplane. Jour. Aero. Sci., vol. 17, no. 3, March 1950,
   pp. 133-148.

3. Anon.: Flying Qualities of Piloted Airplanes. U. S. Air Force
   Specification No. 1815-B, June 1, 1948.

4. Sternfield, Leonard, and Gates, Ordway B., Jr.:   A Simplified Method
   for the Determination and Analysis of the Neutral-Lateral-Oscillatory-
   Stability Boundary. NACA Rep. 943, 1949. (Formerly NACA TN 1727.)

5. Johnson, Joseph L., and Sternfield, Leonard: A Theoretical Investiga-
   tion of the Effect of Yawing Moment Due to Rolling on Lateral
   Oscillatory Stability. NACA TN 1723, 1948.

6. Sternfield, Leonard, and Gates, Ordway B., Jr.:   A Theoretical Analysis
   of the Effect of Time Lag in an Automatic Stabilization System on
   the Lateral Oscillatory Stability of an Airplane. NACA TN 2005,
   1950.

TABLE I

MASS AND AERODYNAMIC CHARACTERISTICS OF A HIGH-SPEED

AIRPLANE AT VARIOUS FLIGHT CONDITIONS

	Condition			
	I	II	III	IV
Altitude, ft	12,000	0	50,000	50,000
W/S_W, lb/sq ft	53	53	53	53
S_W, sq ft	175	175	175	175
b, ft	25	25	25	25
ρ, slugs/cu ft	0.001648	0.002378	0.000361	0.000361
V, ft/sec	458	235	776	1169
Mach number	0.43	0.21	0.80	1.2
l/b	0.80	0.80	0.80	0.80
γ, deg	-19.2	0	0	0
C_L	0.29	0.80	0.49	0.22
μ_b	40	27.7	182	182
K_X^2	0.0181	0.0156	0.0156	0.0159
K_Z^2	0.153	0.156	0.156	0.155
K_{XZ}	-0.0186	0	0.002	-0.006
η, deg	-8.5	0	0.85	-2.55
ϵ, deg	5.2	5.2	3.35	3.35
C_{l_p}, per radian	-0.33	-0.30	-0.33	-0.33
C_{l_r}, per radian	0.37	0.35	0.23	0.15
C_{n_p}, per radian	0.22	-0.05	-0.05	-0.01
C_{n_r}, per radian	-0.984	-0.77	-0.69	-0.67
C_{Y_p}, per radian	0	0	0	0
C_{Y_r}, per radian	0	0	0	0
C_{Y_β}, per radian	-0.79	-0.59	-0.58	-0.57
C_{n_β}, per radian	0.41	0.29	0.25	0.23
C_{l_β}, per radian	-0.23	-0.17	-0.18	-0.11
α, deg	-3.3	5.2	4.2	0.80
ξ, deg	$-3.3 - \frac{\phi}{2}$	$5.2 - \frac{\phi}{2}$	$4.2 - \frac{\phi}{2}$	$0.8 - \frac{\phi}{2}$
$C_{n_{\delta A}}$, per radian	-0.027	-0.027	-0.027	-0.027
$\frac{S_A}{S_R}$	0.20	0.20	0.20	0.20

TABLE II

COMPARISON OF PERIOD AND TIME TO DAMP TO ONE-HALF AMPLITUDE FOR TWO

CENTER-OF-PRESSURE LOCATIONS OF THE AUXILIARY SURFACE

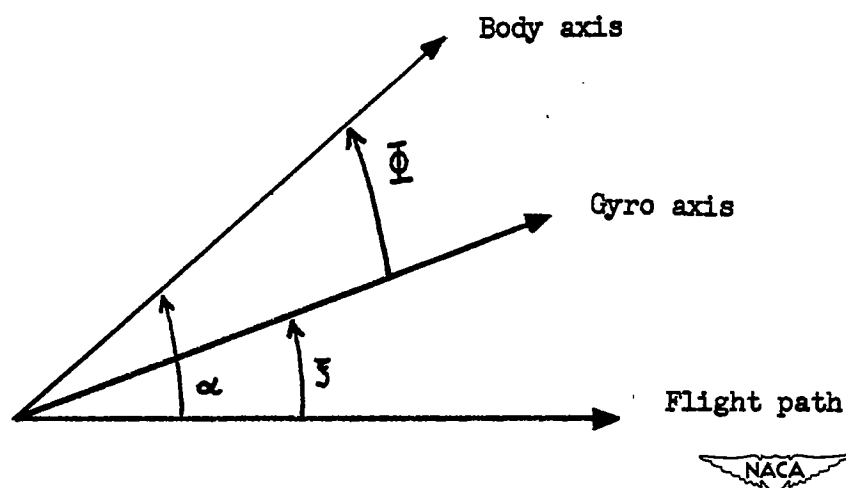| Condition	ϕ	ΔC_{n_r}	ΔC_{n_p}	$(T_{1/2})_1$	$(T_{1/2})_2$	$T_{1/2}$	T_2	P	$(T_{1/2})_1$	$(T_{1/2})_2$	$T_{1/2}$	P	ΔC_{l_r}	ΔC_{l_p}
				$\frac{h}{b}=0$; $\Delta C_{l_r}=\Delta C_{l_p}=0$		Oscillations			$\frac{h}{b}=0.24$		Oscillations			
I	-2.0	-1.98	0.045	1.50	0.26	1.06		2.80	3.48	0.24	1.29	2.52	0.71	-0.016
	2.0	-1.98	.183	-----	-----	{.63 / .64}		{9.34 / 3.74}	3.14	.25	1.07	2.73	.71	-.065
	6.0	-1.98	.321	-----	-----	{3.92 / .36}		{7.06 / 3.09}	2.67	.26	.89	3.03	.71	-.115
	10.2	-1.98	.466	-----	-----	.32	4.22	{8.28 / 2.65}	----	----	{1.25 / .38}	{11.56 / 4.18}	.71	-.167
II	-2.0	-1.01	-.127	3.24	.32	4.50		3.27	5.24	.34	3.83	3.20	.21	.027
	5.2	-1.01	0	2.70	.34	3.20		3.50	4.69	.34	2.77	3.44	.21	0
	10.2	-1.01	.089	2.26	.37	2.80		3.60	4.04	.35	2.15	3.60	.21	-.019
III	-2.0	-3.35	-.363	3.91	.43	4.10		2.83	5.20	.45	9.65	2.95	.76	.08
	2.0	-3.35	-.129	2.64	.58	2.17		2.98	4.09	.52	3.15	3.12	.76	.029
	6.0	-3.35	.105	-----	-----	{1.41 / 1.30}		{21.5 / 3.13}	2.87	.67	1.72	3.33	.76	-.024
	10.2	-3.35	.351	-----	-----	{3.58 / .86}		{11.75 / 3.12}	----	----	{1.60 / 1.02}	{27.8 / 3.6}	.76	-.08
IV	-2.0	-5.05	-.247	4.12	.30	.97		2.45	8.5	.38	.96	2.30	1.44	.071
	2.0	-5.05	.106	2.18	.57	.61		2.63	6.82	.44	.70	2.49	1.44	-.03
	6.0	-5.05	.458	-----	-----	{2.78 / .42}		{12.75 / 2.51}	5.20	.55	.52	2.72	1.44	-.13
	10.2	-5.05	.810	-----	-----	.36	9.0	{12.9 / 2.3}	2.61	1.25	.40	3.83	1.44	-.23

NACA

Figure 1.-. System of axes used in analysis of stability derivatives contributed by autopilot. Arrows denote positive directions.
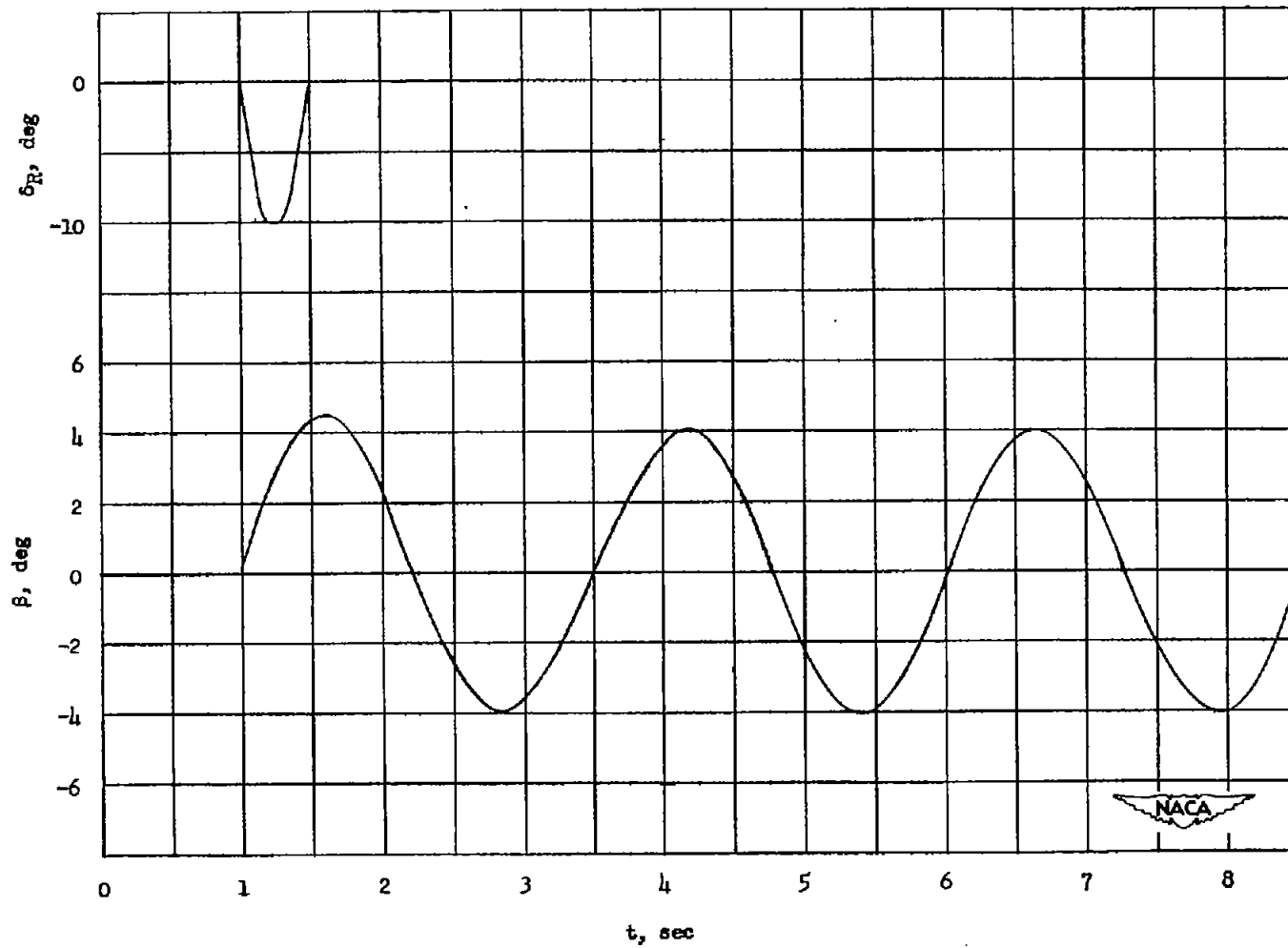
Figure 2.- Motion in sideslip of a typical high-speed fighter airplane at an altitude of 12,000 feet, flaps and gear down, $C_L = 0.29$.
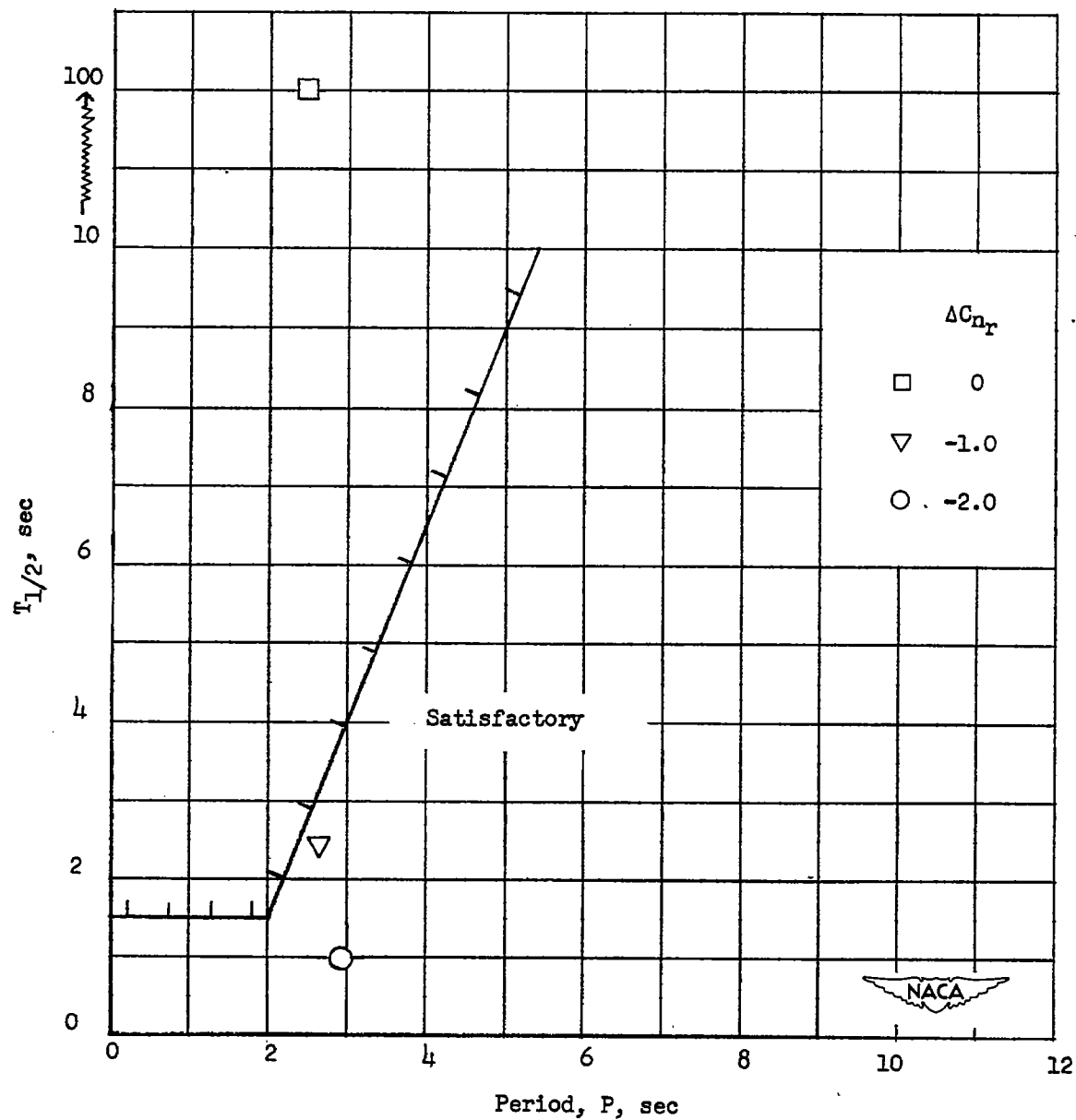
Figure 3.- Effect of C_{n_r} on the damping of the lateral oscillation of the high-speed fighter airplane. Condition I. (See table I.) The period-damping criterion of reference 3 is superimposed.
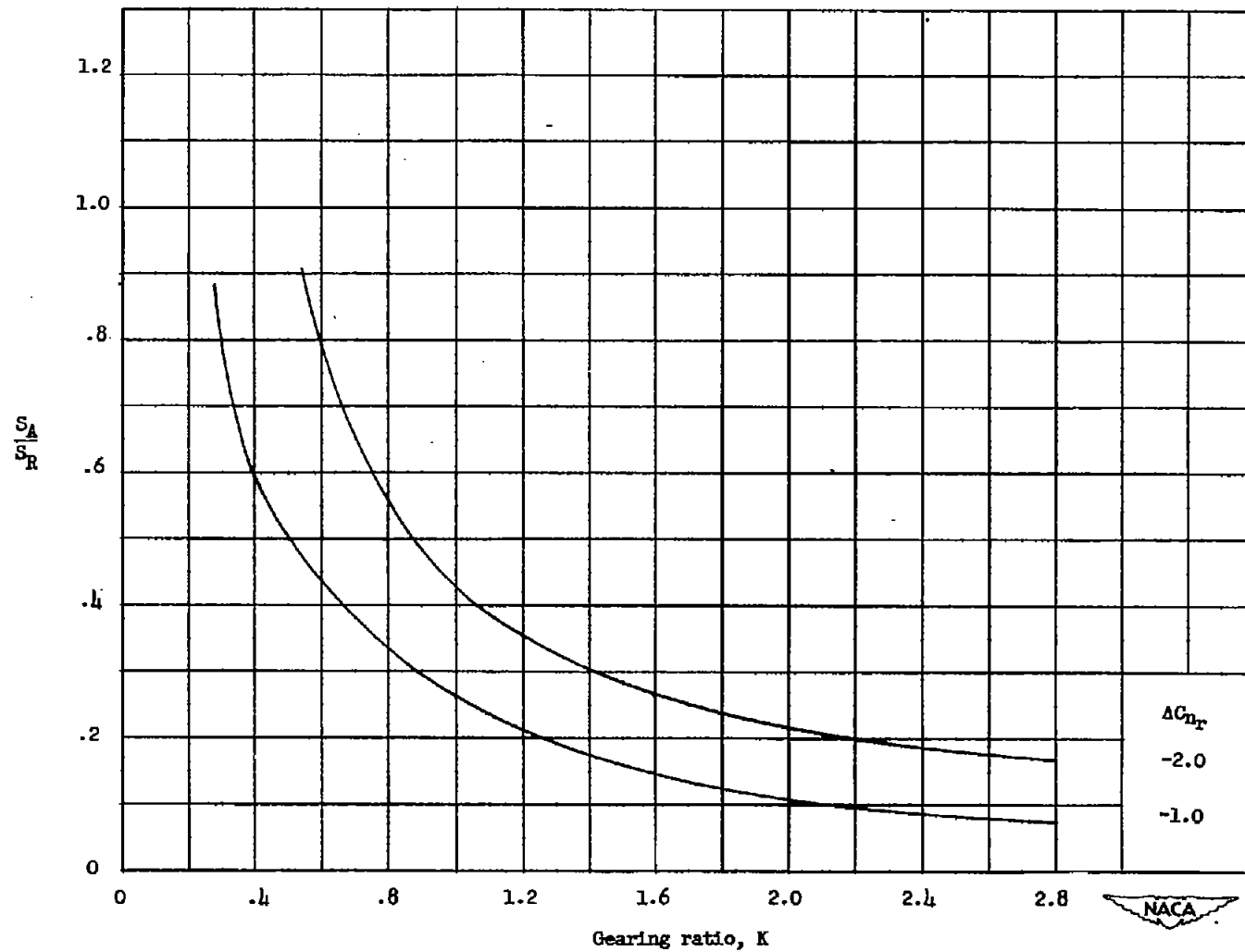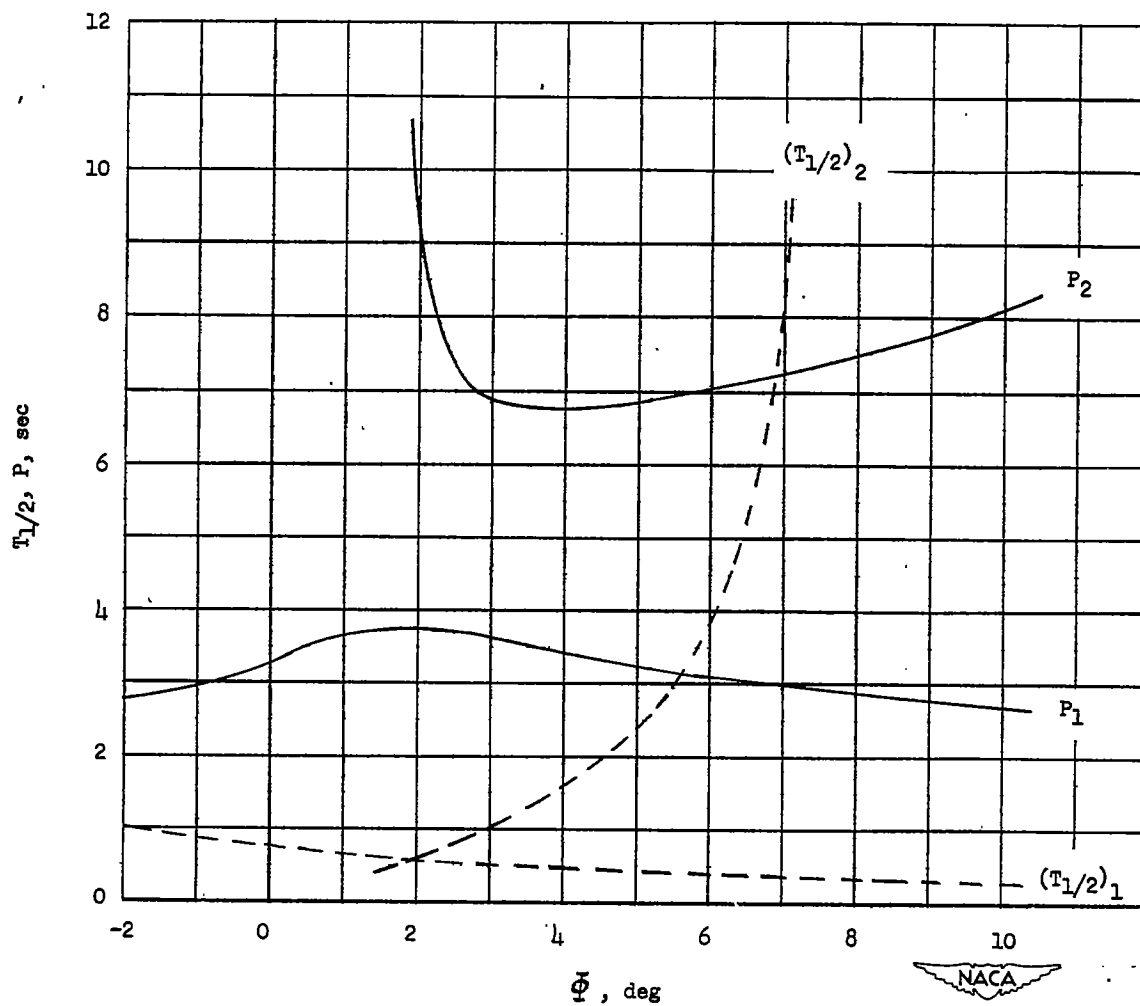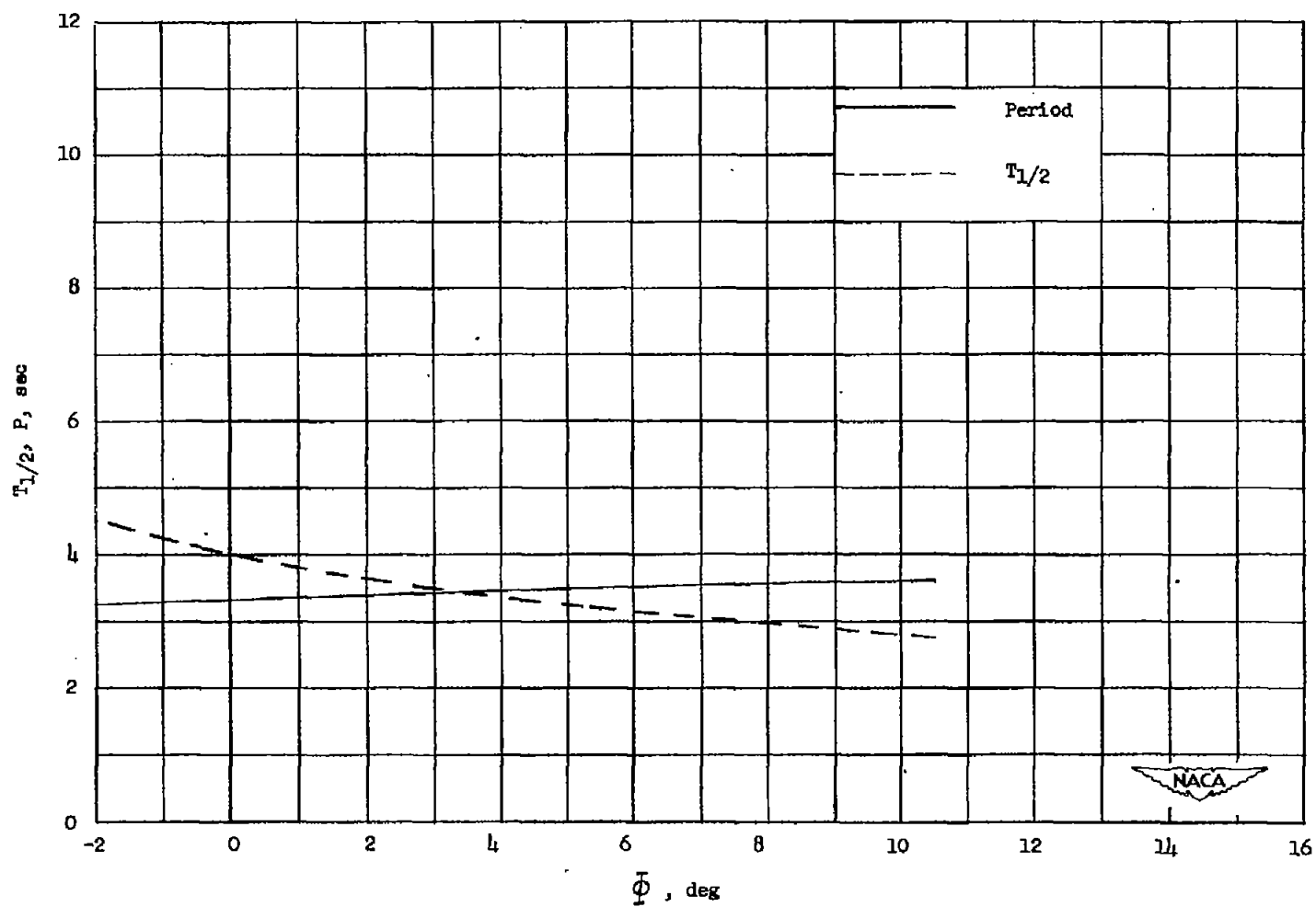
Figure 4.- Combinations of auxiliary surface area and autopilot gearing
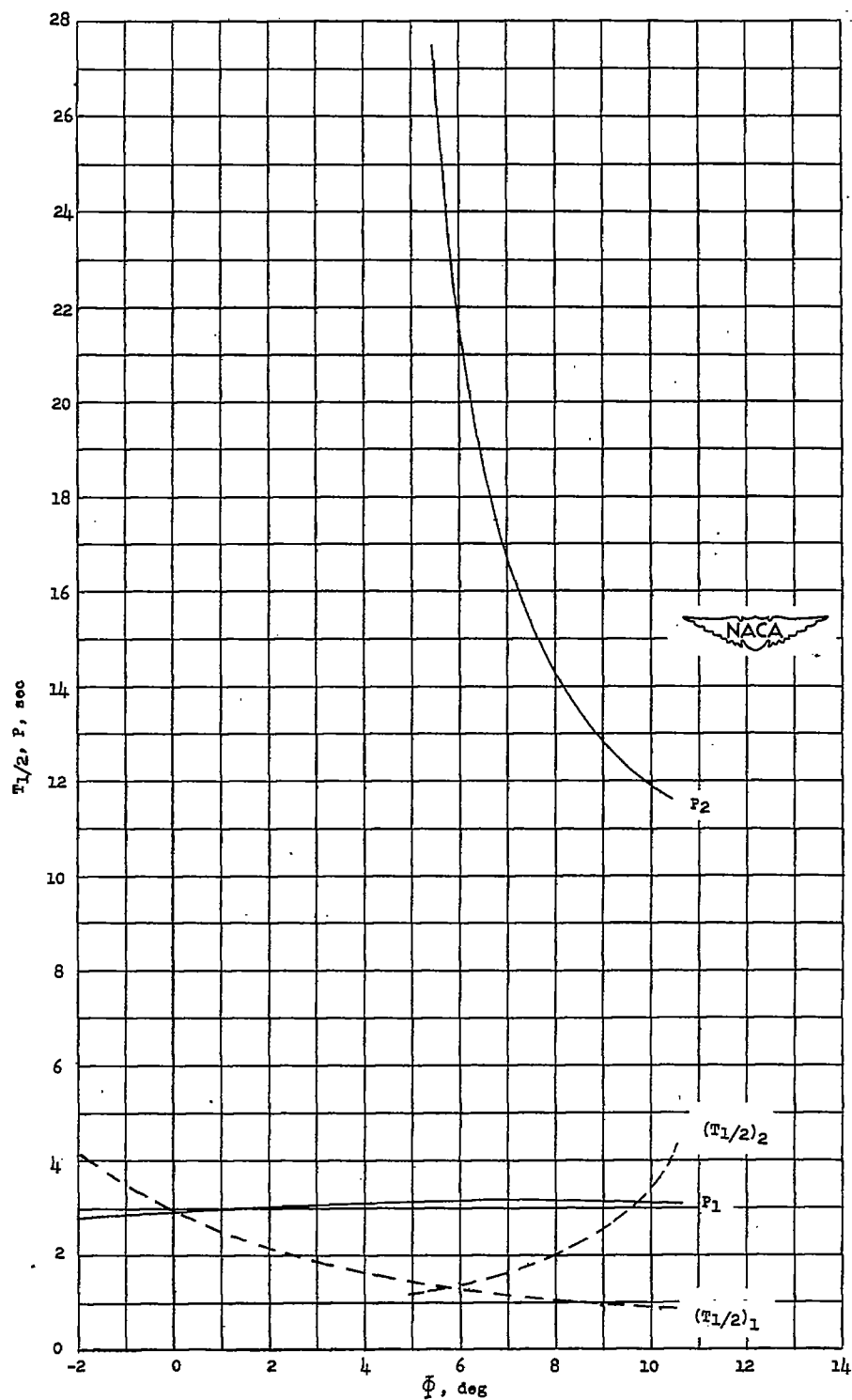ratios necessary to obtain various amounts of ΔC_{n_r}.

(a) Flight condition I. Velocity, 458 feet per second; altitude, 12,000 feet.

Figure 5.- Variation of period and damping of the lateral oscillation of the airplane with autopilot-gyro-axis inclination.
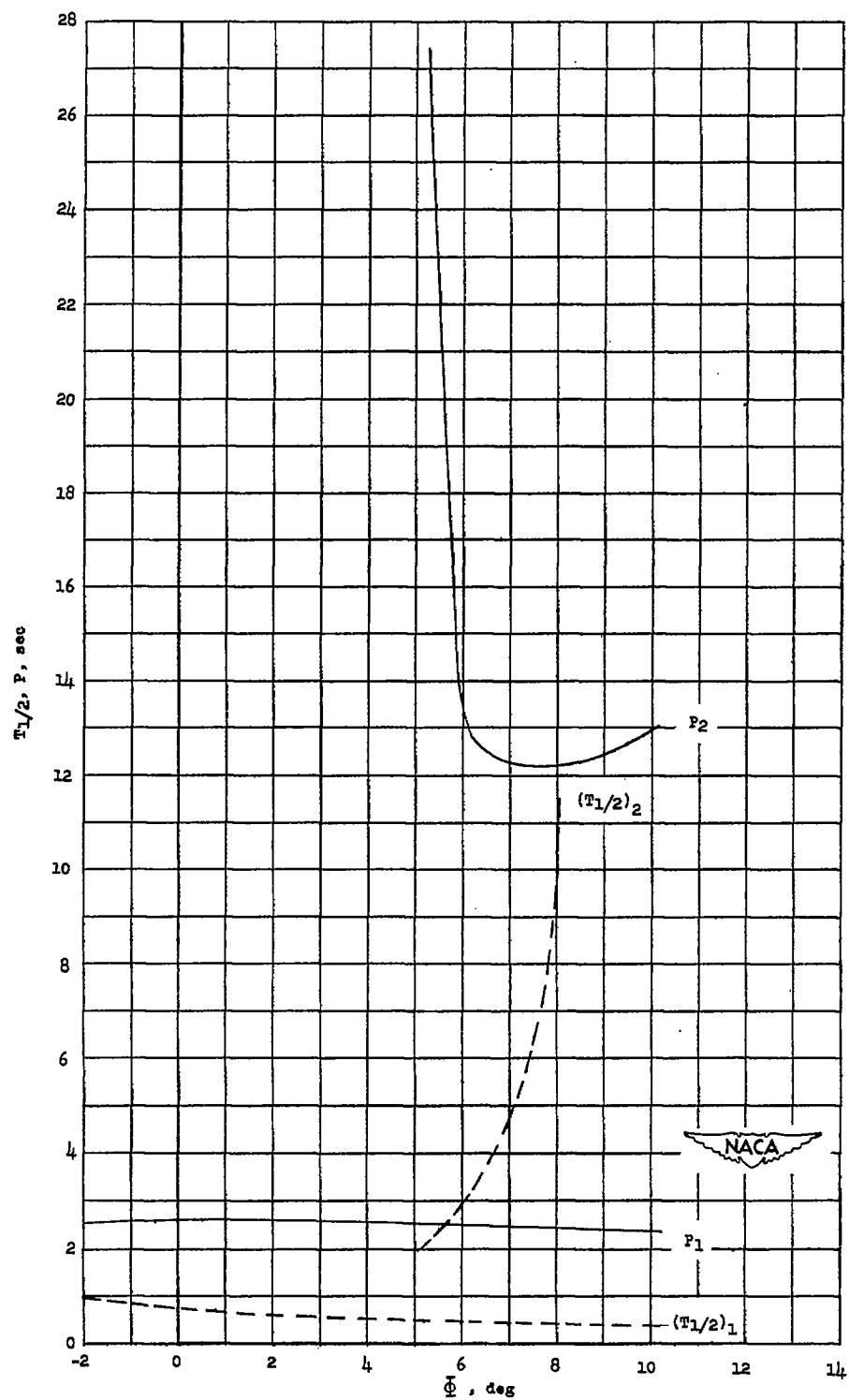
(b) Flight condition II. Velocity, 235 feet per second; altitude,
sea level.

Figure 5.- Continued.

(c) Flight condition III.   Velocity, 776 feet per second; altitude,
50,000 feet.

Figure 5.- Continued.

(d) Flight condition IV. Velocity, 1169 feet per second; altitude, 50,000 feet.
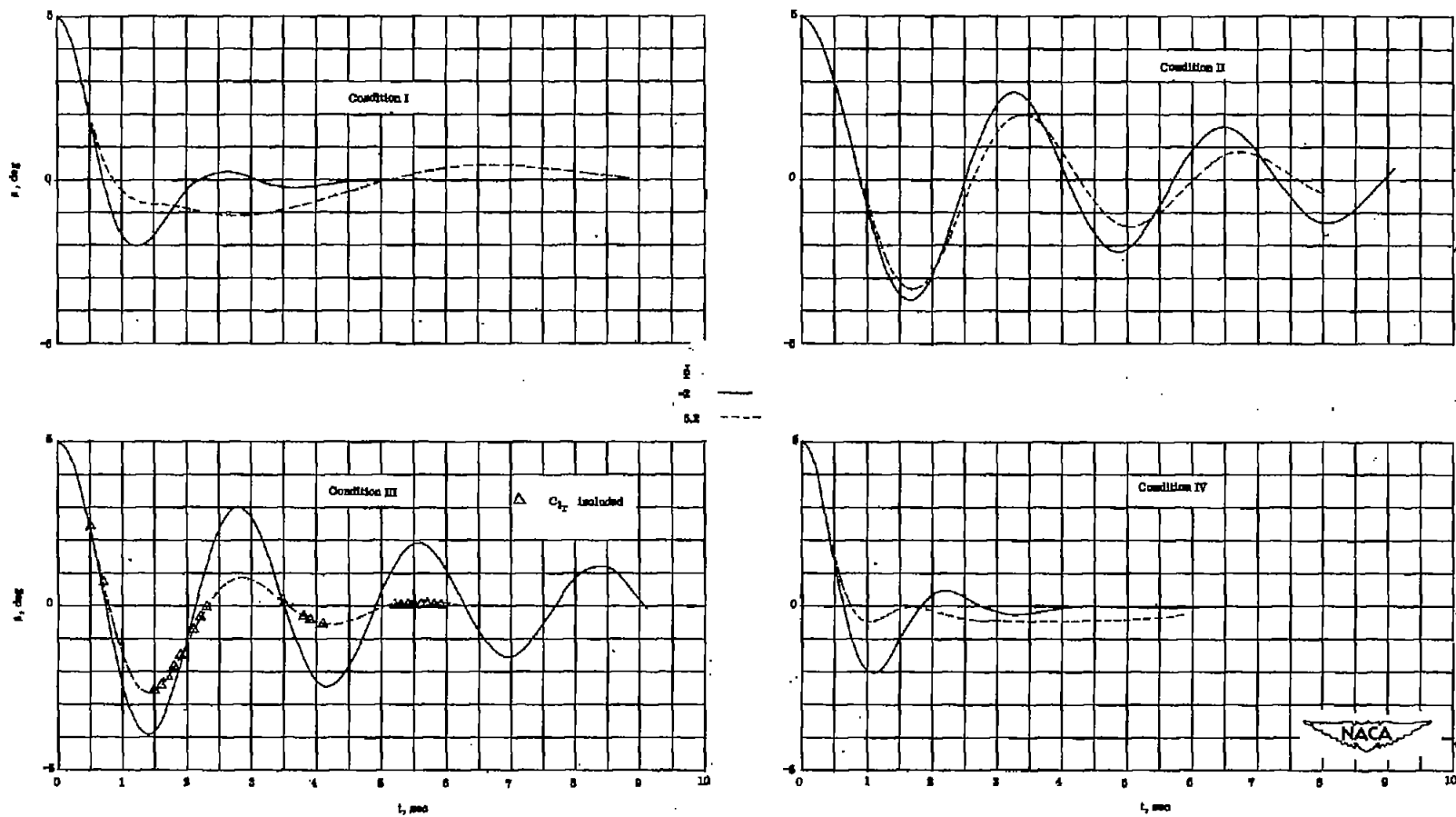
Figure 5.- Concluded.

Figure 6.- Airplane motions in sideslip for several representative flight conditions. $\tau = 0.10$ second.